0026-895X/93/020217-09$03.00/0

MOLECULAR PHARMACOLOGY, 43:217-225

Identification of the Benzomorphan Opiate Binding Site on the Catalytic Subunit of Acetylcholinesterase

BARBARA A. COLEMAN and ROBERT E. OSWALD

Department of Pharmacology, College of Veterinary Medicine, Cornell University, Ithaca, New York 14853

Received August 3, 1992; Accepted November 5, 1992

SUMMARY

The interaction of a benzomorphan opiate with the active site of the catalytic subunit of acetylcholinesterase was studied using photoaffinity labeling. UV irradiation of (−)-*N*-[^{3}H]allylnormetazocine bound to *Torpedo* acetylcholinesterase resulted in covalent incorporation of 60–70% of the bound ligand. The labeled catalytic subunit was subjected to chemical cleavage with cyanogen bromide and proteolytic degradation with trypsin, chymotrypsin, and staphylococcal V8 protease. The resulting peptide fragments were purified by high performance liquid chromatography and sequenced in the gas phase. The label was not stable under the conditions of the sequencing, but a peptide fragment consisting of Gln^{74} to Glu^{82} was reproducibly labeled. These amino acids are located at the rim of a gorge leading to the active site of the enzyme. Molecular modeling studies then demonstrated that these residues can be placed within van der Waals contact of the (−)-*N*-[^{3}H]allylnormetazocine molecule while it is bound to the active site of the enzyme.

AChE is a critical and abundant enzyme in the nervous system of both vertebrates and invertebrates. At cholinergic synapses, it rapidly hydrolyzes the neurotransmitter ACh to terminate its action. This hydrolysis is a result of nucleophilic attack by a serine residue (Ser^{200} in *Torpedo* AChE) and involves a histidine in the charge-transfer complex. Recently, the X-ray structure of AChE from *Torpedo californica* electroplaque was determined by Sussman *et al.* (1), and several unexpected features were present in the active site. Reasoning by analogy with well known serine proteases, an aspartate residue was assumed to complete the catalytic triad. As predicted, a catalytic triad was present in the active site; however, the negative charge was contributed by a glutamate rather than an aspartate residue. Because of the extremely high turnover rate of the enzyme (2), the active site was thought to exist on the surface of the molecule. The crystal structure, though, indicates that the catalytic site is located approximately 16 Å deep in a long gorge lined with hydrophobic residues. Also, an anionic site containing six to nine negatively charged amino acids was postulated to exist to stabilize the charged portion of ACh (3); however, an anionic subsite, *per se*, was not observed in the X-ray structure, because very few charged residues exist in the gorge. Instead, the positive charge of ACh seems to interact with the π electrons of at least one aromatic ring.

This work was supported by grants from the National Institutes of Health (RO1 NS 18660), the Cornell Biotechnology Institute, and Polygen/Molecular Simulations, Inc.

Determination of the protein structure has important implications for the design of anti-AChE drugs. A number of compounds structurally unrelated to ACh bind and inhibit AChE activity and are currently being used clinically (4). Other drugs targeted to specific high affinity receptors also may bind with high affinity to AChE and thus contribute to unwanted side effects. We have previously shown that a benzomorphan opiate, (−)-ANMC (also known as SKF-10,047), readily photoaffinity labels the catalytic subunit of AChE with high affinity and competitively inhibits enzyme activity (5). These and other observations suggested that (−)-ANMC bound to the active site of the enzyme and not the peripheral regulatory site (5). We have investigated the photoaffinity labeling of this morphine derivative by purifying and sequencing labeled peptides in order to understand its binding to and inhibition of AChE. The recent crystallization of the enzyme by Sussman *et al.* (1) has allowed us to propose how ANMC is bound by AChE. This information may shed light on the binding of other drugs used to inhibit AChE activity.

Materials and Methods

Chemicals. Nonradioactive (−)-ANMC and (−)-[^{3}H]ANMC (45.9 Ci/mmol) were provided by the National Institute on Drug Abuse. [^{3}H]DFP (4.4 Ci/mmol) was obtained from DuPont-New England Nuclear. Formic acid, cyanogen bromide, TFA, trypsin, chymotrypsin, MOPS, and NH_4HCO_3 were purchased from Sigma Chemical Co. (St. Louis,

ABBREVIATIONS: AChE, acetylcholinesterase; ACh, acetylcholine; DFP, diisopropylfluorophosphate; DTT, dithiothreitol; EGTA, ethylene glycol-bis(β-aminoethyl ether)-*N*,*N*,*N*′,*N*′-tetraacetic acid; MOPS, 3-(*N*-morpholino)propanesulfonic acid; HPLC, high performance liquid chromatography; FPLC, fast protein liquid chromatography; TFA, trifluoroacetic acid; ANMC, *N*-allylnormetazocine.

MO). HPLC-grade water and acetonitrile were obtained from Fisher (Rochester, NY). Sequencing-grade staphylococcal V8 protease was purchased from Boehringer Mannheim Biochemica (Indianapolis, IN).

Isolation and fragmentation of proteins and peptides. Purified 11 S AChE catalytic subunits were prepared from frozen *Torpedo nobiliana* electroplaque as described by Taylor *et al.* (6), using *m*-aminophenyltrimethylammonium affinity chromatography. Photoaffinity labeling was performed by incubation of 4 mg of purified AChE catalytic subunits with 50 nM (−)-[^{3}H]ANMC, in 10 mM Tris buffer (pH 7.5) containing 100 mM NaCl and 40 mM $MgCl_2$, at room temperature for 45 min in polystyrene plates and subsequent irradiation with UV light (254 nm) for 20 sec at a distance of 6 cm (5). In order to determine the effects of salt and divalent cations on AChE binding, photoaffinity labeling of AChE was also done after extensive dialysis of the enzyme against 50 mM MOPS, 5 mM EGTA. MOPS (50 mM) was adjusted to pH 7.5 using 33 mM NaOH. [^{3}H]DFP labeling was carried out as described by MacPhee-Quigley *et al.* (7). (−)-[^{3}H]ANMC- or [^{3}H]DFP-labeled catalytic subunits were also prepared for enzymatic cleavage as described by MacPhee-Quigley *et al.* (7). Specifically, [^{3}H]DFP- or (−)-[^{3}H]ANMC-labeled 11 S AChE was dialyzed overnight against 50 mM NH_4HCO_3 to remove unreacted label. After lyophilization, labeled protein was resuspended to 1 mg/ml with 6 M guanidine·HCl in 0.1 M Tris·HCl, pH 8.0. DTT was added to a 2-fold molar excess over total cysteine residues, and the mixture was incubated at 50° for 3 hr. Cysteines were acetylated with iodoacetate to prevent disulfide bond reformation, by addition of a 2-fold molar excess over DTT. The reaction was stopped by addition of a 10-fold molar excess of DTT before overnight dialysis as described above. The protein was lyophilized again before cleavage by CNBr. CNBr fragments were generated by resuspension of the protein in 500 μl of 70% formic acid, addition of 1–3 mg of cyanogen bromide, and incubation at 25° for 36–48 hr. Cleaved enzyme was lyophilized again to remove formic acid. After resuspension in 200 μl of 50 mM NH_4HCO_3 buffer (pH 8.3), the fragments were separated on a Pharmacia FPLC Superose 12B gel filtration column, in resuspension buffer (50 mM NH_4HCO_3, pH 8.3), at 0.25 ml/min at 4°. Aliquots were removed from each 0.8-ml fraction and assayed for radioactivity. Protein absorbance was monitored at 280 nm during FPLC separations or at 214 nm during HPLC purifications. Data were digitized and stored on an Apple Macintosh 512K computer, using a program developed in the laboratory.

(−)-[^{3}H]ANMC-labeled radioactive peaks corresponding to protein absorbance peaks at 280 nm were pooled for reverse phase chromatography using HPLC. After lyophilization, pooled peaks were resuspended with 5% aqueous acetonitrile containing 0.1% TFA as an ion-pairing agent, sonicated briefly to aid resuspension, and loaded onto a C-18 column (YMC ODS-C18). CNBr fragments were loaded in 10% acetonitrile. After 5 min, the concentration was increased in linear fashion to 25% over 5 min. Radioactive peptides were then purified with a 25–30% linear gradient over 30 min. All HPLC gradients contained 0.1% TFA as an ion-pairing agent.

Trypsin fragments were generated by incubation of labeled dialyzed AChE with 0.1% (w/w) trypsin overnight at 37°. An additional 0.1% (w/w) trypsin was subsequently added for 2 hr at 37°. Fifty micrograms of chymotrypsin were added to the total trypsin digest or 5 μg were added to purified trypsin fragments resuspended in 100 mM Tris buffer (pH 8.0). Chymotrypsin digests were incubated at room temperature for 2 hr. Digests were lyophilized before size exclusion chromatography by FPLC as described for CNBr-generated peptides. Radioactive pools were subsequently loaded onto an HPLC C-18 column in 5% acetonitrile and eluted with a linear gradient to 50% over 50 min.

Staphylococcal V8 protease was added either to labeled intact AChE or to CNBr-cleaved, HPLC-purified peptides resuspended in 25 mM phosphate buffer (pH 7.8). Acetonitrile (5%) was added to stimulate enzyme activity. Incubations were done at 25° for 18 hr. HPLC separations of size-fractionated radioactive pools were done on a C-18 column. Samples were loaded in 10% acetonitrile for 2 min before the concentration of acetonitrile was increased to 25% over 2 min. The elution gradient was then run and consisted of a linear gradient from 25 to 30% acetonitrile over 54 min.

Amino acid analysis and peptide sequencing. Amino acid analysis and protein sequencing were done by the Cornell University Biotechnology Center, using standard methods (8, 9). Amino acid analysis was performed using a Water's PicoTag System. Gas-phase protein sequencing was accomplished with an Applied Biosystem model 470A sequencer with on-line phenylthiohydantoin analysis.

Molecular modeling. A Silicon Graphics 4D/220GTX computer running Quanta and CHARMm software was used to study the interaction of ANMC with the active site of AChE. The coordinates for the X-ray structure of AChE were provided by Dr. J. Sussman (Weizmann Institute of Science, Rehovot, Israel) (1).

Results

Purification of labeled peptides. Asymmetric AChE catalytic subunits were purified to near-homogeneity, as determined by sodium dodecyl sulfate-polyacrylamide gel electrophoresis and protein absorbance profiles of AChE run on an FPLC Superose 12B sizing column (Fig. 1A). The catalytic subunits were covalently labeled with either (−)-[^{3}H]ANMC or [^{3}H]DFP in buffer containing 100 mM NaCl, 40 mM $MgCl_2$, and 10 mM Tris (pH 7.5). After labeling, the proteins were denatured, reduced, alkylated with iodoacetate to prevent reformation of disulfide bonds, and dialyzed. Labeled enzyme was digested with CNBr in 70% formic acid, and fragments were separated on a gel filtration column (Superose 12B) that resolves proteins between 1000 and 300,000 daltons. CNBr cleaves carboxyl-terminally to methionine residues and should yield 17 fragments, ranging in length from 7 to 100 amino acids (Fig. 2), according to the sequence published by Schumacher *et al.* (10). Ten of these fragments are predicted to contain between 20 and 40 amino acid residues. Thus, a major protein peak would be expected to correspond to the [^{3}H]DFP-labeled peptide of 33 amino acids. The protein absorbance of cleaved and uncleaved AChE is shown in Fig. 1A, with the elution profiles for radioactivity in Fig. 1B. [^{3}H]DFP-labeled protein showed a single major peak of radioactivity, corresponding to a major protein peak. (−)-[^{3}H]ANMC radioactivity showed two major peaks and a shoulder that also corresponded to the major protein peak. Peak II (Fig. 1B) varied in location and intensity between preparations. Upon HPLC chromatographic analysis, the majority of radioactivity from this peak eluted either in the void volume of the column (despite varied loading conditions) or just after the column void volume, but without corresponding to any protein absorbance at 214 nm. Despite numerous attempts, no peptides could be recovered from peak II, as determined by sequence analysis. Peak III eluted at the column salt volume and predominantly results from instability of the radioactive label upon exposure to 70% formic acid for 48 hr, because this high level of radioactivity in the salt volume was not seen when proteolytic cleavages were done near neutral pH. No radiolabeled peptides were observed in this pool. The majority of (−)-[^{3}H]ANMC radioactivity associated with specific peptide incorporation was found in peak I.

Peak I was lyophilized for further purification. HPLC reverse phase chromatography of [^{3}H]DFP- and (−)-[^{3}H]ANMC-labeled fragments indicated that radioactivity overlapped but peaked at 28% and 28.5% acetonitrile, respectively, using a steeper elution gradient than was later used for isolation of individual fragments. Initial HPLC purifications of CNBr-cleaved, (−)-[^{3}H]ANMC-labeled protein from peak I demon-

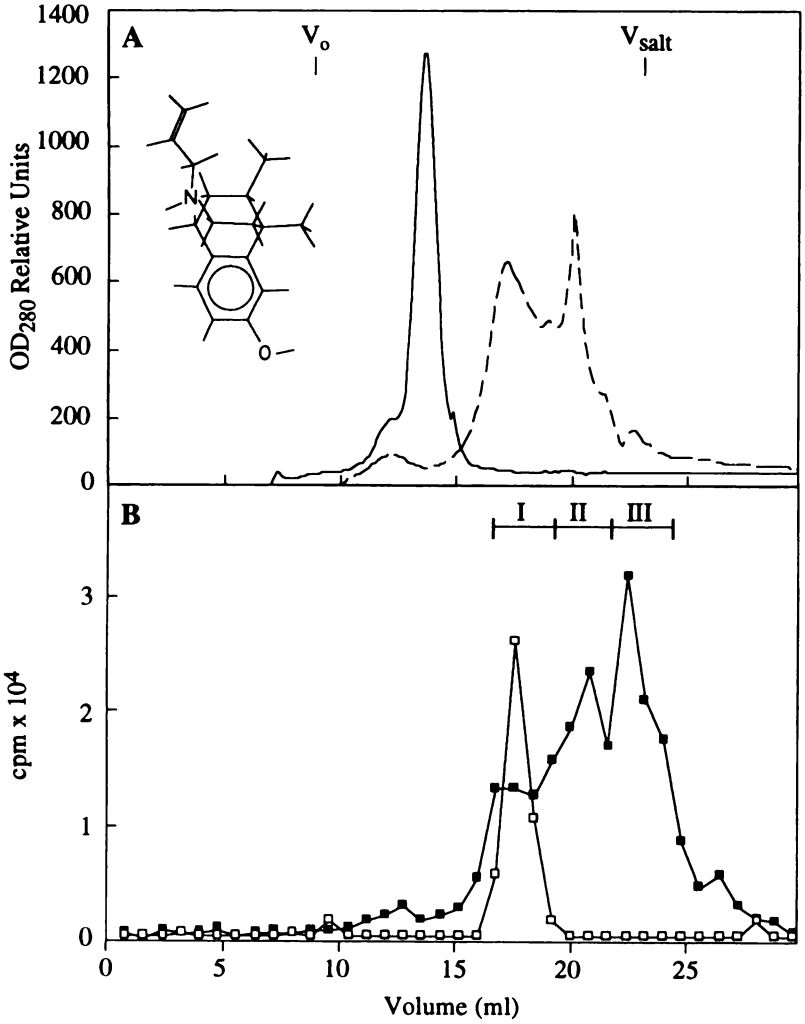

Fig. 1. Gel filtration chromatography on Superose 12B of purified *Torpedo* AChE before and after cleavage by CNBr. A, Absorbance profile at 280 nm. – – –, Cleaved enzyme; ——, uncleaved enzyme. *Inset*, structure of (−)-ANMC. B, Radioactivity profiles of [^{3}H]DFP-labeled (□) and (−)-[^{3}H] ANMC-labeled (■) enzyme after CNBr cleavage.

strated a number of peptide fragments. Successive chromatography using a two-step gradient, as described in Materials and Methods, resulted in one radioactive peptide peak (Fig. 3), which was consistently isolated from each of six such preparations. However, sequence analysis of the single (−)-[^{3}H]ANMC peak indicated the presence of two peptide fragments in approximately equal concentrations. Unexpectedly, neither fragment corresponded to that which would contain the active site Ser^{200}. One peptide (fragment A) began with Arg^{44} and would be expected to terminate at Met^{83}. The second fragment (fragment B) spanned Asp^{380} to Met^{405}. Although the entire amino acid sequence of fragment B could be determined, the sequence of fragment A generally ceased after Pro^{53}, the 10th amino acid of the peptide. Amino acid analysis of the mixed fragments demonstrated levels of phenylalanine, proline, glutamine, and glutamate that could not be accounted for by fragment B and the first 10 residues of fragment A, suggesting that all of fragment A was present but could not be sequenced due to a block at Trp^{54}. Careful subfractionation of a peak similar to that shown in Fig. 3 from one preparation resulted in purification of radioactivity in fragment A only, although sequencing again terminated prematurely after Pro^{53}. This indicated that the fragments were not cross-linked but rather coeluted coincidentally. In two paired labeling studies, an identical HPLC peptide peak was generated by CNBr cleavage of AChE exposed to UV in the presence and absence of drug. Results of amino acid sequencing indicated the presence of the same two fragments seen previously, confirming that (−)-ANMC did not cross-link the peptides. Sequencing of fragment A from unlabeled preparations again terminated prematurely, a further indication that (−)-ANMC was not responsible for the block at Trp^{54}. No radioactivity was recovered from any of the sequencing cycles, suggesting that the labeled amino acid existed in the unsequenced portion of fragment A or that the label was unstable under the conditions used for sequencing. Attempts were made to identify the type of residue labeled by collecting fractions during total amino acid analysis. No radioactivity was found corresponding to any amino acid peak; however, radioactivity was recovered in fractions preceding elution of the first amino acid, indicating that the radioactive labeling was unstable under the harsh conditions used to hydrolyze peptide bonds (6 N HCl at 150° for 90 min).

To define the labeling site further, trypsin and chymotrypsin fragments were generated. Digests were run on a Sepharose 12B column and three peaks of radioactivity were observed (data not shown). These peaks were individually pooled for subsequent separation by HPLC as described in Materials and Methods. Three radioactively labeled peptides, corresponding to peaks 1, 2, and 3 in Fig. 4, were found in all of the size-fractionated pools because of incomplete resolution by the gel filtration column, although a different fragment predominated in each pool. Each radioactive peak observed during HPLC

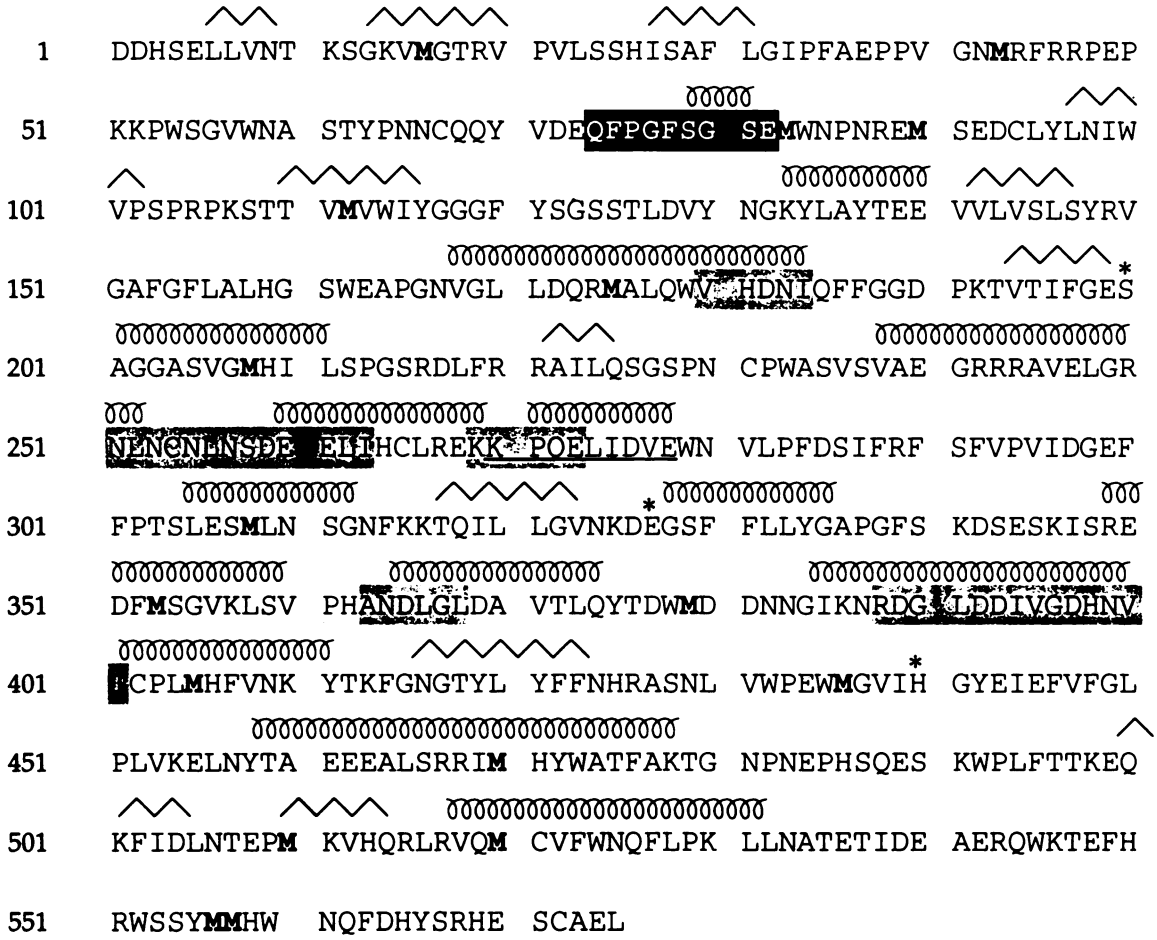

Fig. 2. Amino acid sequence of the catalytic subunit of *Torpedo* AChE. The amino acid sequence is taken from the work of Schumacher *et al.* (10) and the elements of secondary structure from the crystal structure reported by Sussman *et al.* (1). *Looped lines*, regions of α-helix; *angled lines*, regions of β-strand. Methionine residues are shown in *bold* to indicate the CNBr cleavage sites. *Boxed residues* (*black* or *gray*), sequences that were labeled by (−)-[^{3}H]ANMC in at least two different preparations. *Black box*, main site of (−)-[^{3}H]ANMC incorporation. *Underlined amino acids*, fragments that correspond to a peripheral regulatory site as described by Weise *et al.* (26). *, Residues involved in the catalytic triad.

fractionation of Sepharose 12B pools was collected. These were ultimately pooled according to their elution times; peptide peaks 1, 2, and 3 (Fig. 4) required two, three, and five chromatographic separations, respectively, as described in Materials and Methods, to achieve purification (i.e., a symmetrical absorbance peak that corresponded to elution of radioactivity). Sequence analysis of peak 3 indicated that it is the AChE fragment consisting of amino acids Val^{71} to Trp^{84}. This peptide comprises the carboxyl-terminal portion of fragment A isolated from CNBr digestions. No other peptides were present in this peak, confirming that (−)-ANMC labeled a portion of fragment A that could not be sequenced from CNBr-generated fragments.

Sequencing of the trypsin/chymotrypsin-digested peak 1 indicated that it was composed mostly of the protein fragment Asn^{251}-Ile^{263}, although a small amount (<15%) of a contaminating peptide, Ala^{157}-Gly^{169}, was also detected. Peak 2 resulted from a short peptide of amino acids Val^{180} to Ile^{184}. None of these fragments corresponded to portions of fragment B from CNBr digests, further indicating that the labeled peptide present in the peak shown in Fig. 3 was fragment A. Recovery of radiolabeled fragments that could not be isolated from CNBr digests probably resulted from greater recovery of radioactivity in general because of the lack of formic acid treatment.

In order to localize the labeling site of (−)-[^{3}H]ANMC further, limited proteolysis with staphylococcal V8 protease was undertaken. V8 cleaves specifically after glutamate and aspartate residues under the conditions used (11, 12). AChE was photoaffinity labeled, cleaved with CNBr, and separated on a gel filtration column as described above. A radioactive fragment similar to that shown in Fig. 3 was isolated and digested with V8 protease. Fig. 5 shows the change in protein and radioactivity elution profiles before treatment with the enzyme and after two HPLC purifications after protease digestion. Sequence analysis from different preparations indicated that the radioactive fragment consisted of amino acids Gln^{74} to Glu^{82}, again corresponding to the carboxyl terminus of fragment A. One preparation cleaved only with V8 contained a fragment corresponding to amino acids Lys^{269} to Glu^{273}, in addition to Gln^{74} to Glu^{82}. No radioactivity was recovered in any of the Edman degradation cleavage cycles of V8-generated peptides.

Effects of reduced ionic strength. Sodium and magnesium ions have long been known to activate AChE activity (13–15). Therefore, the effects of reduced ionic strength on photoaffinity labeling of AChE by (−)-ANMC were investigated by sequencing peptide fragments of enzyme labeled in buffer containing 50 mM MOPS (pH 7.5) and 5 mM EGTA. The Na^+ concentration from pH adjustments with NaOH was 33 mM. Essentially no free divalent cations were present, because of

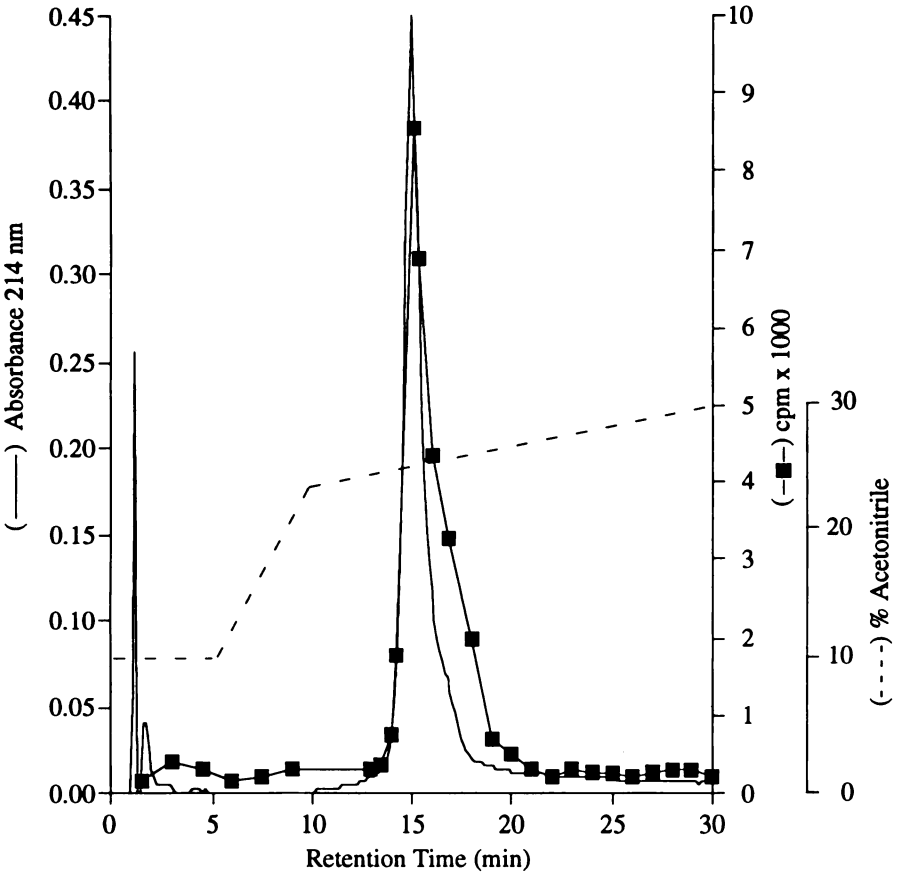

Fig. 3. Purification of CNBr peak I using HPLC reverse phase chromatography. The absorbance profile at 214 nm and the total radioactivity recovered are shown and are the final result of three chromatographic runs.

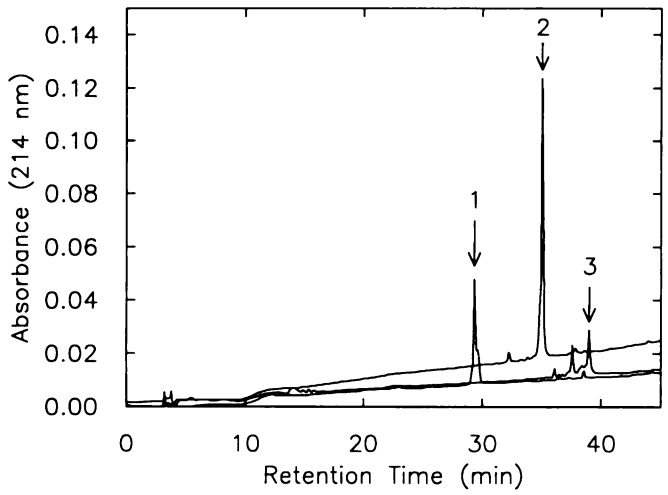

Fig. 4. Purified trypsin/chymotrypsin AChE fragments labeled with (–)-[^{3}H]ANMC and purified by reverse phase HPLC. Labeled AChE was treated with trypsin and chymotrypsin and the peptides were separated by FPLC on Sepharose 12B. The three peaks of radioactivity were then purified by reverse phase HPLC on a C-18 column, and the final separations are shown here. The absorbance at 214 nm is plotted. *Arrows*, peaks of radioactivity.

extensive dialysis against buffer containing 5 mM EGTA. Results of three paired photolabeling studies showed that, in reduced salt buffer lacking divalent cations, AChE incorporated only 31 ± 15% (mean ± standard deviation) of the radioactivity covalently bound in higher ionic strength medium. The protein was digested with trypsin and chymotrypsin to avoid loss of the label as a result of treatment with formic acid. Chromatographic separation of the peptides labeled in reduced ionic strength buffer demonstrated that a number of radioactive fragments could be isolated from any single preparation. Sequences containing radioactivity under these labeling conditions included amino acids 180–187, 251–263 (both also seen in preparations labeled under higher ionic strength conditions), 268–281 (also seen with V8-digested AChE labeled in salt- and divalent cation-containing buffer), 204–206, 217–220, 363–370, 363–371, 359–368, 388–401, 405–407, and 569–575. Overlapping sequences from radioactive fragments isolated at least twice from different preparations are summarized in Fig. 2. Notably, in six preparations labeled in medium with lower salt concentrations and without divalent cations, no peptides could be isolated that corresponded to residues 74–82, a major site of labeling seen in the presence of higher NaCl and $MgCl_2$ concentrations. Thus, the efficiency of photoaffinity labeling of residues 74–82 appeared to be decreased under reduced ionic strength conditions. This might result from a conformational change in the enzyme, reduced hydrophobic interactions important for labeling at this site, or a combination of these factors.

Instability of incorporated radioactivity. Increased amounts of radioactivity were occasionally recovered during some sequencing cycles, independently of the labeling conditions. In most instances, however, radioactivity was highest in the first cycle and steadily decreased to background levels. This further indicated that the label was unstable under conditions used for Edman degradation. Attempts to discern which amino acid was labeled were made using a variety of other methods, although none was successful in determining the exact site of incorporation. The difficulty may stem from acid sensitivity of

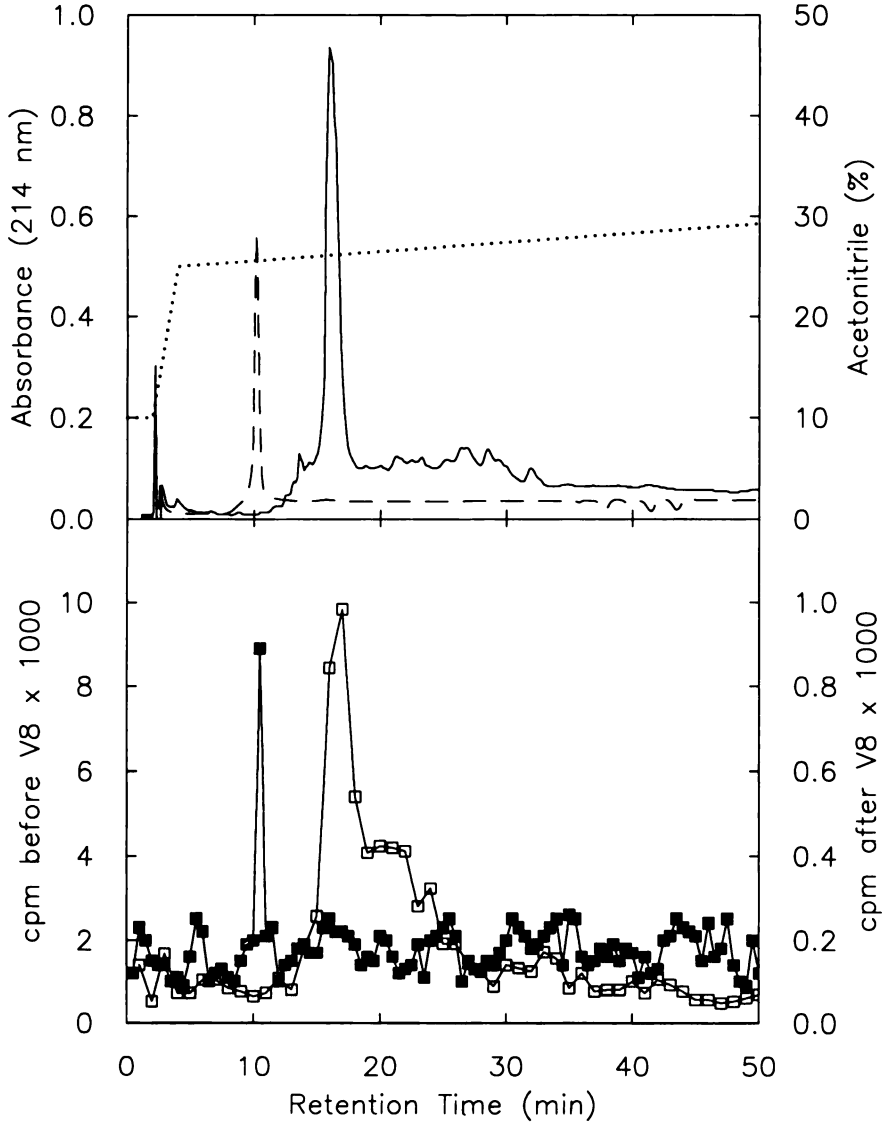

Fig. 5. V8 protease fragments generated from the labeled CNBr fragment. A, Absorbance profile at 214 nm for the labeled fragment before (——) and after (– – –) protease treatment. · · · ·, Percentage of acetonitrile. B, Radioactivity profile of labeled fragments before (□) and after (■) V8 protease treatment.

the covalent bond formed during UV irradiation. Notably, in CNBr-cleaved preparations using 70% formic acid, 52 ± 1.5% (mean ± standard deviation of four preparations) of the total radioactivity eluted in the salt volume of the column. In trypsin and chymotrypsin digestions, where cleavage occurred at pH 7–8, only 15 ± 2.9% (mean ± standard deviation of three preparations) of the label was found in the salt volume. H^+ exchange is known to occur with allylic groups under acidic conditions (16) and could result in exchange of the terminal radioactive protons. Either proton exchange or an acid-sensitive bond between (−)-[^{3}H]ANMC and AChE would account for the large amount of free radioactivity seen after prolonged exposure to 70% formic acid and the inability to recover radioactively labeled amino acids during amino acid analysis and sequencing.

Modeling of (−)-ANMC binding to the active site. These results suggest that photoaffinity labeling of AChE by (−)-ANMC was more efficient in high ionic strength buffer. Approximately 3 times more radioactivity was incorporated when 40 mM $MgCl_2$ and 100 mM NaCl were present than when sodium was reduced to 33 mM and Mg^{2+} was eliminated. When AChE was labeled in high ionic strength buffer, fragments containing amino acids 74–82 were consistently isolated and peptides corresponding to other amino acids could sometimes be isolated as well. In buffer where the salt concentration was reduced and divalent cations were not present, a variety of fragments representing a number of labeling sites were recovered. None, however, corresponded to amino acids 72–84. Examination of the structure of AChE shows that amino acids 72–84 are located at the top of the gorge leading to the catalytic site of the enzyme (see Fig. 6). Carbamylcholine inhibits (−)-[^{3}H]ANMC binding and photoaffinity labeling. Edrophonium, a ligand specific for the catalytic site, was shown to displace (−)-[^{3}H]ANMC binding (5). Phosphorylation of the active site Ser^{200} by DFP (5) markedly reduced the binding affinity of (−)-ANMC and inhibited photoaffinity labeling. Thus, (−)-ANMC is likely to bind in the active site gorge and label residues 74–82 from within the cleft. The fragments labeled in lower ionic strength were all on the surface of the enzyme, presumably reflecting an interaction with surface anionic sites.

A molecular model of (−)-ANMC was constructed using the ChemNote program in Quanta (Polygen/Molecular Simula-

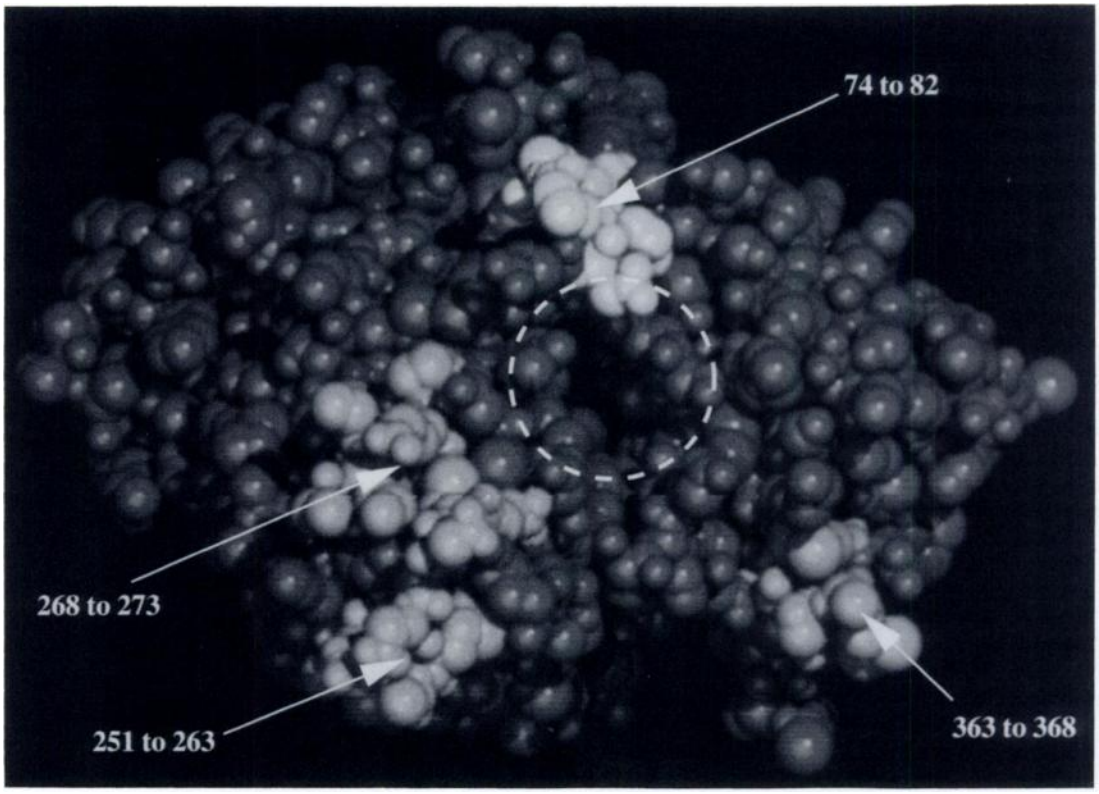

Fig. 6. Space-filling model of AChE with labeled residues indicated. Shown here is a space-filling model generated using Quanta (Polygen) with the peptides that were labeled by (−)-[^{3}H]ANMC. *Light gray*, major site of labeling (residues 74–82); *medium gray*, location of peptides labeled by (−)-[^{3}H]ANMC in at least two different preparations. *Dashed circle*, mouth of the gorge leading to the active site.

tions, Inc.). The conformation of the drug was optimized by energy minimization in vacuum using the CHARMm force field. The molecular model of (−)-ANMC was manually docked in the AChE gorge such that the phenol ring was located within hydrogen-bonding distance of Ser^{200}, with the allyl groups oriented toward residues 74–82. Phosphorylation of Ser^{200} dramatically reduced ANMC binding and eliminated photoaffinity labeling (5), indicating that the drug interacted with either Ser^{200} or His^{440}, or both. The catalytic serine and histidine residues are believed to be hydrogen bonded; thus, interactions of (−)-ANMC with either residue would be affected by serine phosphorylation. Although the mechanisms of photoaffinity labeling by (−)-ANMC are unknown, some involvement of the allyl group of ANMC seems likely because the unsaturated double bond is more easily disrupted than are σ bonds between carbon and other elements (17). For molecular modeling studies, the phenol ring of (−)-ANMC was positioned toward the catalytic residues, with the quaternary amine oriented toward the opening of the gorge, by analogy with the proposed binding of ACh to the enzyme (1).

Energy minimization to remove unfavorable contacts was done in vacuum using the CHARMm force field. Three stages of minimization were used; 1) the entire AChE molecule was constrained and the position of ANMC was allowed to vary, 2) ANMC and the side chains of Phe^{75} and Phe^{78} were allowed to vary, and 3) ANMC and all aromatic side chains within the gorge were allowed to vary. One hundred cycles of steepest descent minimization were followed by 200 cycles of Adopted-Basis Newton Raphson minimization (Quanta; Polygen/Molecular Simulations, Inc.). This procedure provides a plausible orientation of ANMC in the binding site but is not necessarily the optimal structure because of the presence of other minima in the energy surface, the fact that not all resuides were allowed to vary, the absence of explicit water molecules, and potential differences between the crystal and solution structures of AChE. The resultant structure (Fig. 7) placed the -OH group of (−)-ANMC in a position to hydrogen bond with both Ser^{200} and His^{440}. The nitrogen atom, which is largely protonated under the conditions of labeling (as determined from the proton NMR spectrum at 300 MHz, obtained with a Bruker WM-300 spectrometer), was surrounded by three of the aromatic amino acids that line the gorge. The aromatic rings of Trp^{84}, Phe^{330}, and Tyr^{334} were all <5 Å from the nitrogen and were oriented such that the π electrons of each ring faced the positively charged atom (Fig. 7). Hydrogen atoms from the double bond of (−)-ANMC reached within 3.5 Å of an aromatic carbon (Phe^{75}) and within 3.9 Å of Ser^{81}. Multiple orientations of the side chain of ANMC are possible due to free rotation around the C-N bond and also around the single C-C bond of the allyl group. The orientation of the side chain depicted in Fig. 7 predicts that the terminal portion of the allyl group can extend to within van der Waals distance from Phe^{75} and Ser^{81}.

Discussion

The studies described here were undertaken to investigate the site and mechanism of (−)-ANMC interaction with AChE. (−)-ANMC is capable of photoaffinity labeling AChE with very high efficiency (>60% of the bound radioactivity is covalently incorporated) (5) and the labeling is modulated by ACh derivatives and monovalent and divalent cations. After the labeling,

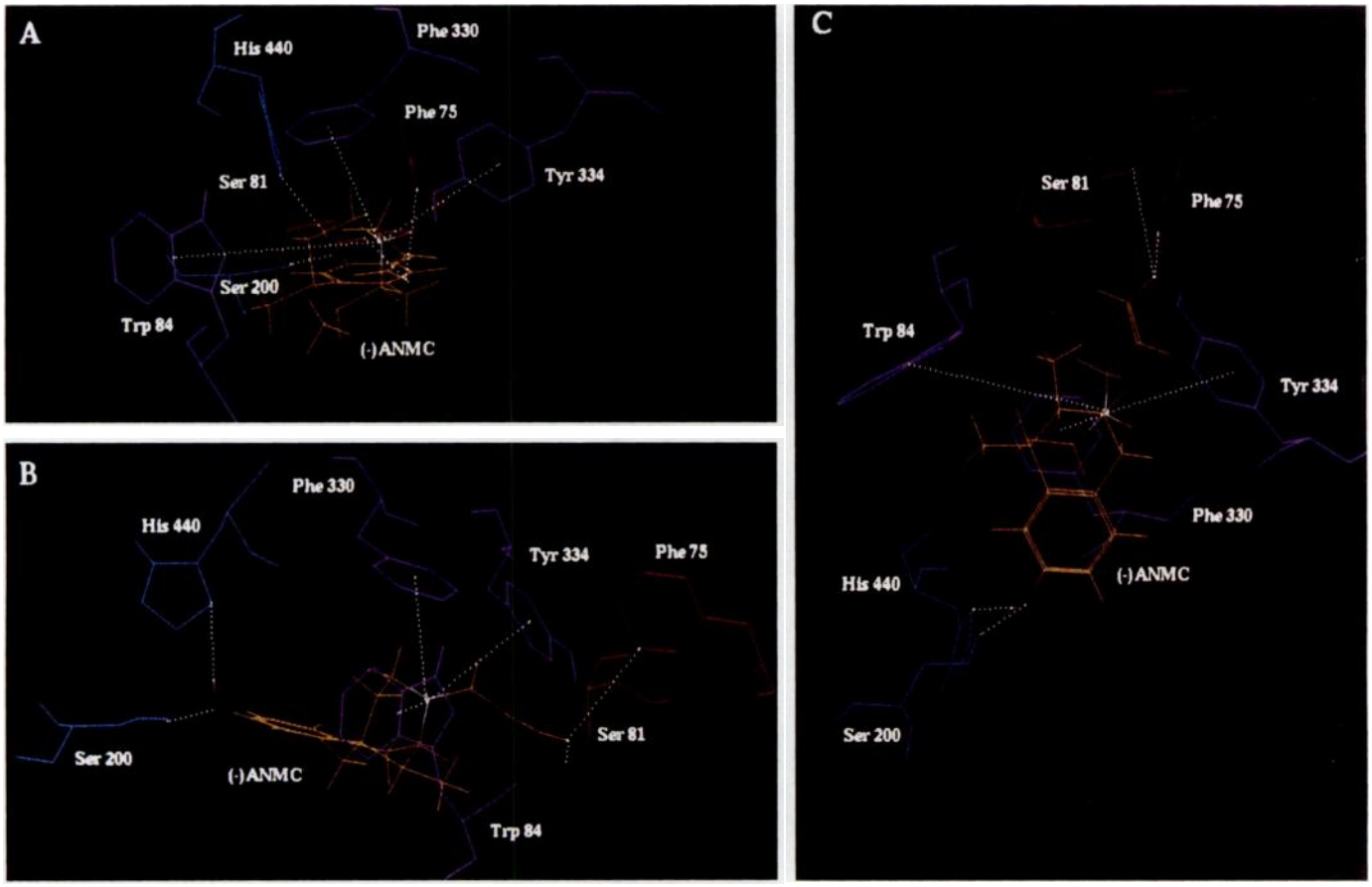

Fig. 7. Proposed binding site of (−)-[^{3}H]ANMC on AChE, as suggested from the photoaffinity labeling studies and molecular modeling. Shown are selected features of the active site of AChE with the (−)-ANMC molecule in its energy-minimized position, from three different angles. A, A view from the top of the gorge looking down toward the active center; the gorge runs horizontally in B and vertically in C. *Blue*, catalytic residues; *purple*, aromatic amino acids that could stabilize the positively charged nitrogen; *red*, amino acids of the labeled peptide that can approach within van der Waals distance of (−)-ANMC; *yellow*, (−)-ANMC.

the enzyme was subjected to either proteolytic degradation or CNBr cleavage. Under ionic strength conditions approaching those found physiologically, a peptide fragment containing amino acids Gln^{74} to Glu^{82} was consistently isolated, independently of cleavage mechanisms. Because no labeled amino acid was detected in Edman degradation, presumably because of the instability of the label, the conclusion that this peptide is the major site of label is based on the fact that it was purified and sequenced after four different cleavage protocols (CNBr alone, CNBr followed by V8 protease, V8 protease alone, and trypsin/chymotrypsin). Because of the instability of the label, the possibility that other peptides may be specifically labeled and represent physiologically relevant sites of action cannot be ruled out. Based on the crystal structure of the enzyme (1), this position corresponds to the mouth of the gorge that leads to the active site. When the ionic strength was reduced and free divalent cations were eliminated from the buffer, the efficiency of photoaffinity labeling dropped by approximately 60%. A number of peptides, all of which were on the surface of the enzyme, were labeled under these conditions.

The binding of (−)-ANMC to AChE can be regulated by agents that interact with a peripheral anionic binding site (5). The existence of a peripheral anionic ligand binding site that affects AChE activity in an allosteric manner was first suggested by Changeux (18). Since then, much evidence has accumulated to establish the existence of an anionic regulatory site on AChE distinct from the catalytic site. A variety of organic cationic ligands have been shown to bind to this peripheral site (18–22). Ligand binding to the peripheral site induces conformational changes in the active site of the enzyme (19, 22, 23). These conformations are spectroscopically distinct depending on the peripheral site ligand bound (23), indicating that occupation of this anionic allosteric site can induce more than a single conformation at the active center. Divalent cations also interact with the peripheral anionic site (20), with alkaline earth metals (Mg^{2+}, Ca^{2+}, and Mn^{2+}) activating enzyme activity and transition metals (Cu^{2+}, Zn^{2+}, etc.) inhibiting enzyme activity. The fact that the residues at the mouth of the gorge leading to the active site could be labeled only in physiological salt solution (including Mg^{2+}) is consistent with the activation of the enzyme by divalent cations. Our previous results indicated that the simultaneous addition of (−)-ANMC and carbamylcholine stimulated a dramatic increase in the rate of (−)-ANMC association measured both by radioligand binding and by photoaffinity labeling (5, 24). Subsequently, over the course of the next 60 sec, carbamylcholine decreased the binding and photoaffinity labeling to control levels. In light of the structure of AChE and the results presented in this paper, one potential

interpretation of these findings is that the function of the peripheral anionic site is to activate the enzyme by inducing a conformational change that increases the accessibility to the active site.

Computer modeling studies of ANMC binding at the active site of AChE suggest several interesting points. The hydroxyl group of (−)-ANMC was manually positioned near the catalytic Ser^{200}. Energy minimization subsequently positioned (−)-ANMC between Ser^{200} and His^{440}, thereby permitting hydrogen-bonding with both amino acids. The positively charged quaternary amine of (−)-ANMC, like that of ACh (1), is expected to be oriented toward the opening of the gorge. This effectively centers it ~5 Å from each of three aromatic amino acids (Trp^{84}, Phe^{330}, and Tyr^{334}) whose planar rings are oriented facing the charge (see Fig. 7). Several lines of evidence suggest that the charged portion of ACh, and other quaternary cationic ligands, can be stabilized in the gorge by these aromatic residues. Photoaffinity labeling experiments have implicated Trp^{84} as part of the "anionic subsite" (25). Molecular modeling studies by Sussman *et al.* (1) also suggested involvement of Trp^{84} in the binding of ACh. Using enzyme isolated from *Electrophorus*, Phe^{330} was labeled as part of the active site of AChE (26). Chemical modification studies further predicted tyrosine residues near the catalytic site (27). The binding of cholinergic ligands has been proposed by Dougherty and Stauffer (28) to involve stabilization of the quaternary ammonium by electrostatic interactions with π electrons from aromatic amino acids. They based this hypothesis on photoaffinity labeling studies of AChE and the ACh receptor, the choline binding site of an immunoglobulin, and their own "guest-host" experiments. Indeed, an artificial receptor consisting primarily of aromatic residues was shown to bind ACh with a K_d of 50 μM (28). The distance for amino-aromatic interactions was predicted by Burley and Petsko (29) to be between 3.4 Å and 6 Å, based on their studies of positively charged amino acid side chain stabilization in proteins. As suggested by our computer modeling studies, the positively charged nitrogen would be surrounded by three aromatic residues whose distance (~5 Å) and orientation are in good agreement with predictions for stabilization of charge by cation-π interactions and synthetic receptor models. An anionic subsite consisting primarily of aromatic amino acids also helps explain the hydrophobic nature of the site demonstrated in numerous binding studies.

In summary, (−)-[^{3}H]ANMC was previously shown to bind to the active center of AChE and to inhibit its activity in a competitive manner. Combined with the results of photoaffinity labeling studies presented here, we propose that, in the presence of high magnesium and sodium concentrations, (−)-ANMC labels residues 74–82 from within the catalytic gorge, where its binding is stabilized by hydrogen bonding with catalytic residues and by interactions of its charged nitrogen with the π electrons of aromatic residues Trp^{84}, Phe^{330}, and Tyr^{334}.

Acknowledgments

The authors would like to thank Dr. Gregory A. Weiland, Dr. Tadhg Begley, and Ms. Joanna Feltham (Cornell University) for helpful discussions.

References

1. Sussman, J., M. Harel, F. Frolow, C. Oefner, A. Goldman, L. Toker, and I. Silman. Atomic structure of acetylcholinesterase from *Torpedo californica*: a prototypic acetylcholine-binding protein. *Science (Washington D. C.)* **253**:872–879 (1991).
2. Rosenberry, T. L. Acetylcholinesterase. *Adv. Enzymol. Related Areas Mol. Biol.* **43**:103–218 (1975).
3. Nolte, H.-J., T. L. Rosenberry, and E. Neumann. Effective charge on acetylcholinesterase active sites determined with the ionic strength dependence of association rate constants with cationic ligands. *Biochemistry* **19**:3705–3711 (1980).
4. Chatellier, G., and L. Lacomblez, on behalf of Groupe Francais d'Etude de la Tetrahydroaminoacridine. Tacrine (tetrahydroaminoacridine; THA) and lecithin in senile dementia of the Alzheimer type: a multicentre trial. *Br. Med. J.* **300**:495–499 (1990).
5. Coleman, B., L. Michel, and R. E. Oswald. Interaction of a benzomorphan opiate with acetylcholinesterase and the nicotinic acetylcholine receptor. *Mol. Pharmacol.* **32**:456–462 (1987).
6. Taylor, P., J. W. Jones, and N. M. Jacobs. Acetylcholinesterase from *Torpedo*: characterization of an enzyme species isolated by lytic procedures. *Mol. Pharmacol.* **10**:78–92 (1974).
7. MacPhee-Quigley, K., P. Taylor, and S. Taylor. Primary structures of the catalytic subunits from two molecular forms of acetylcholinesterase. *J. Biol. Chem.* **260**:12185–12189 (1985).
8. Heinrikson, R. L., and S. C. Meredith. Amino acid analysis by reverse-phase high performance liquid chromatography: precolumn derivatization with phenylisothiocyanate. *Anal. Biochem.* **136**:65–74 (1984).
9. Hunkapiller, M. W., K. Granlund-Moyer, and N. W. Whiteley. Gas-phase protein/peptide sequencer, in *Methods of Protein Microcharacterization: A Practical Handbook* (J. E. Shively, ed.). Human Press, Clifton, NJ, 223–247, (1986).
10. Schumacher, M., S. Camp, Y. Maulet, M. Newton, K. MacPhee-Quigley, S. S. Taylor, T. Friedmann, and P. Taylor. Primary structure of *Torpedo californica* acetylcholinesterase deduced from its cDNA sequence. *Nature (Lond.)* **319**:407–409 (1986).
11. Houmard, J., and G. R. Drapeau. Staphylococcal protease: a proteolytic enzyme specific for glutamoyl bonds. *Proc. Natl. Acad. Sci. USA* **69**:3506–3509 (1972).
12. Drapeau, G. R., Y. Boily, and J. Houmard. Purification and properties of an extracellular protease of *Staphylococcus aureus*. *J. Biol. Chem.* **247**:6720–6726 (1972).
13. Nachmansohn, D. Actions of ions on cholinesterase. *Nature (Lond.)* **145**:513–514 (1940).
14. Tomlinson, G., B. Mutus, and I. McLennan. Activation and inactivation of acetylcholinesterase by metal ions. *Can. J. Biochem.* **59**:728–735 (1981).
15. Hofer, P., U. P. Fringeli, and W. H. Hopff. Activation of acetylcholinesterase by monovalent (Na^+, K^+) and divalent (Ca^{2+}, Mg^{2+}) cations. *Biochemistry* **23**:2730–2734 (1984).
16. March, J. *Advanced Organic Chemistry: Reactions, Mechanisms, and Structure.* McGraw-Hill Book Co., New York (1968).
17. Noller, C. R. *Chemistry of Organic Compounds.* W. B. Saunders Co., Philadelphia (1965).
18. Changeux, J. P. Responses of acetylcholinesterase from *Torpedo marmorata* to salts and curarizing drugs. *Mol. Pharmacol.* **2**:369–392 (1966).
19. Mooser, G., and D. S. Sigman. Ligand binding properties of acetylcholinesterase determined with fluorescent probes. *Biochemistry* **13**:2299–2307 (1974).
20. Taylor, P., and S. Lappi. Interaction of fluorescence probes with acetylcholinesterase: the site and specificity of propidium binding. *Biochemistry* **14**:1989–1997 (1975).
21. Berman, H. A., J. Yguerabide, and P. Taylor. Fluorescence energy transfer on acetylcholinesterase: spatial relationship between peripheral site and active center. *Biochemistry* **19**:2226–2235 (1980).
22. Berman, H. A., W. Becktel, and P. Taylor. Spectroscopic studies on acetylcholinesterase: influence of peripheral-site occupation on active-center conformation. *Biochemistry* **20**:4803–4810 (1981).
23. Epstein, D. J., H. A. Berman, and P. Taylor. Ligand-induced conformational changes in acetylcholinesterase investigated with fluorescent phosphonates. *Biochemistry* **18**:4749–4810 (1979).
24. Oswald, R. E., L. Michel, and J. Bigelow. Mechanism of binding of a benzomorphan opiate to the acetylcholine receptor from *Torpedo* electroplaque. *Mol. Pharmacol.* **29**:179–187 (1986).
25. Kieffer, B., M. Goeldner, C. Hirth, R. Aebersold, and J.-Y. Chang. Sequence determination of a peptide fragment from electric eel acetylcholinesterase, involved in the binding of quaternary ammonium. *FEBS Lett.* **202**:91–96 (1986).
26. Weise, C., H.-J. Kreienkamp, R. Raba, A. Pedak, A. Aaviksaar, and F. Hucho. Anionic subsites of the acetylcholinesterase from *Torpedo californica:* affinity labelling with the cationic reagent *N,N*-dimethyl-2-phenylaziridinium. *EMBO J.* **9**:3885–3888 (1990).
27. Blumberg, S., and I. Silman. Inactivation of electric eel acetylcholinesterase by acylation with *N*-hydroxysuccinimide esters of amino acid derivatives. *Biochemistry* **17**:1125–1131 (1978).
28. Dougherty, D. A., and D. A. Stauffer. Acetylcholine binding by a synthetic receptor: implications for biological recognition. *Science (Washington D. C.)* **250**:1558–1560 (1990).
29. Burley, S. K., and G. A. Petsko. Amino-aromatic interactons in proteins. *FEBS Lett.* **203**:139–143 (1986).

Send reprint requests to: Robert E. Oswald, Department of Pharmacology, College of Veterinary Medicine, Cornell University, Ithaca, NY 14853.